Optica Applicata, Vol. XLII, No. 4, 2012
DOI: 10.5277/oa120402

Non-diffraction fringes produced by thin biprism

ZHOU LIPING, GAN JIANGHONG*, XU LONG

School of Mechanical Science and Engineering, Huazhong University of Science and Technology, Wuhan 430074, China

*Corresponding author: ganjh@smail.hust.edu.cn

Thin biprism can form non-diffraction fringes when it is illuminated by coherent plane wave and the non-diffraction fringes have long focal length and uniform intensity distribution. Geometrical optics characteristic of thin biprism is analyzed. Non-diffraction field produced by thin biprism at the Fresnel zone is deduced with exact Fresnel integral and an approximation representation is obtained by the stationary phase method. Numerical calculation is utilized to investigate the properties of non-diffraction fringes and evaluate the influence of the diffractive field caused by rectangle aperture's square edge on the fringes. An experiment is setup to observe the intensity of the non-diffraction fringes.

Keywords: fringe, interference, non-diffraction, stationary phase method, thin biprism.

1. Introduction

Axicon, a term coined by McLeod, designates a wide class of optical elements with figures of revolution that focus light from a point source on the axis onto its segment [1]. Since then, there has been a considerable interest in the design and analysis of diffractive axicons that produce a focal segment with the uniform optical distribute along the propagation axis within a specified region because of their utility for metrological application [2–5]. The focal segment within the specified region is closely related to non-diffraction Bessel beams and other propagation-invariant fields [6–8]. Referring to axicons, Fresnel biprism with suitable phase retardation can form stable optical fringes with long distance, narrow spacing. Owing to their many potential applications [9] in metrology, interferometry and laser technology, the analysis, design and numerical simulation of general thin biprism are important. However, to our knowledge, thin biprism as a simple wave-front-dividing element is only used to measure the wavelength and refractive index accuracy [10, 11] till now.

The aim of this paper is to analyze the properties of the fringes generated by interference of the diffractive field of a normal thin biprism, when it is illuminated by a plane wave. In Section 2, we use the geometric optics method to analyze the interference fringes characteristic of two plane waves divided by the thin biprism as a simple

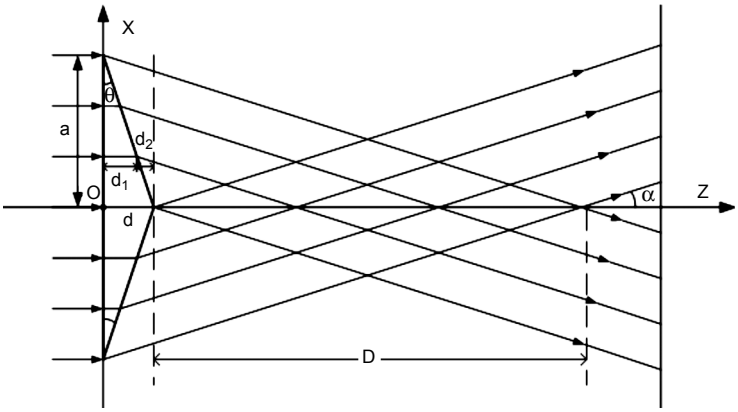

Fig. 1. Geometric optics path of thin biprism and the notations.

splitter element [12]. In Section 3, the scalar diffraction theory [13] with paraxial approximation is utilized to induce the diffractive field distribution, and stationary phase method [4, 14, 15] is applied to give an approximation expression of the Fresnel integral. In Section 4, numerical calculation is utilized to analyze the fringes characteristics at the diffractive field, and the influence of the diffractive field caused by the square edge of the aperture is evaluated. In Section 5, an experiment is set up to observe the fringes distribution and non-diffraction property produced by a plane wave illuminating a thin biprism. The brief conclusions are given in Section 6.

2. Geometric optics of thin biprism

Figure 1 shows a cross-sectional view of the thin biprism with the refractive index n, refractive angle θ and maximum thickness d, where d is sufficiently smaller than the observation distance. The Z axis is defined as the original propagation of a collimated beam; the X axis is defined along the wege angle direction vertical to the Z axis on the plane. The thin biprism having axial symmetrical structure with a rectangle aperture (size $2a \times 2b$) has been considered. The thin biprism is illuminated normally by a monochromic plane wave proceeding in the z direction. The electric field ($\mathbf{E}$) of the plane wave with unit amplitude is expressed as follows:

$$\mathbf{E}(x, y, z) = \exp(\mathbf{i}kz) \tag{1}$$

where $k = 2\pi/\lambda$ is the propagation constant and λ is the wavelength.

The plane wave is divided into two coherence waves by thin biprism. According to Snell's law, these two waves are deflected toward x and $-x$ direction, respectively, and the complex-amplitude distribution of the two waves are given by

$$\mathbf{E}_{\mathbf{a}}(x, y, z) = \exp\left\{\mathbf{i}k\left[z\cos(-\alpha) + x\cos\left(\frac{\pi}{2} + \alpha\right)\right]\right\} \tag{2a}$$

$$\mathbf{E_b}(x, y, z) = \exp\left\{\mathbf{i}k\left[z\cos(-\alpha) + x\cos\left(\frac{\pi}{2} - \alpha\right)\right]\right\} \tag{2b}$$

where $\mathbf{E_a}$, $\mathbf{E_b}$ are the complex-amplitudes of the field with deflected angle $(\pi/2 + \alpha)$ and $(\pi/2 - \alpha)$ along the X axis, respectively; $\alpha = [\text{asin}(n\sin\theta) - \theta]$ is the deflected angle, when θ is small enough, the deflected angle can be simplified as

$$\alpha = (n - 1)\theta \tag{3}$$

Consequently, the intensity distribution on the interference zone is given by

$$I(x, y, z) = \left|\mathbf{E_a}(x, y, z) + \mathbf{E_b}(x, y, z)\right|^2 =$$

$$= 2\left[1 + \cos(2kx\sin\alpha)\right] \approx 2\left[1 + \cos(2kx\alpha)\right] \tag{4}$$

The length of the maximum focal segment along the Z axis is given by

$$D = a(\cot\alpha - \tan\theta) \tag{5}$$

At any observation plane $z_1 < D$, substituting the Eq. (3) into Eq. (4), we obtain the intensity distribution

$$I(x, y, z_1) = 2\left\{1 + \cos\left[2k(n - 1)\theta x\right]\right\} \tag{6}$$

The fringes spacing at the observation plane can be obtained from Eq. (6),

$$d_p = \frac{\lambda}{2\alpha} = \frac{\lambda}{(n - 1)\theta} \tag{7}$$

From Eq. (6) and Eq. (7), we can conclude that the fringes have equal spacing and the intensity has sinusoidal distribution along the x direction on the observation plane, the spacing and the intensity distribution have no relationship with the propagation distance z. That is to say, the fringes distribution has non-diffraction property at the interference area. In order to explain the diffraction property, the scalar diffraction theory, with the paraxial approximation, is used to analyze the diffractive patterns.

3. Diffraction patterns analysis of thin biprism

Consider a thin biprism, showed as Fig. 2, with a transmittance function given by

$$t(x_1, y_1) = \exp\left[-i(n - 1)k\left|x_1\right|\theta\right] \tag{8}$$

The thin biprism is illuminated by a normally incident monochromatic plane wave with the unit amplitude and the wavelength λ. According to the Fresnel approximation

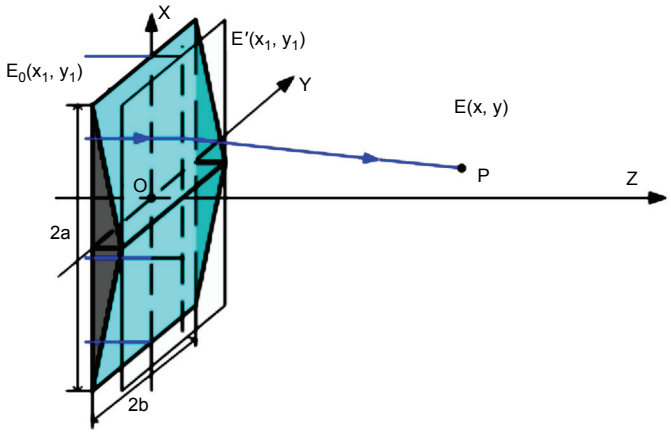

Fig. 2. Scalar diffraction of thin biprism with rectangle aperture and definition of the coordinate systems.

and taking into account the rectangle aperture, the complex-amplitude distribution at an observation plane situated at the distance z_1 ($0 < z_1 < D$) from the biprism can be written

$$E(x,y) = \frac{\exp(ikz_1)}{i\lambda z_1}\iint_{\Sigma} t(x_1,y_1)\exp\left\{\frac{ik}{2z_1}\left[(x-x_1)^2+(y-y_1)^2\right]\right\}\mathrm{d}x_1\mathrm{d}y_1 =$$

$$= \frac{\exp\left[ik(z_1+nd)\right]}{i\lambda z_1}\int_{-a}^{a}\exp\left\{ik\left[\frac{(x-x_1)^2}{2z_1}-(n-1)|x_1|\theta\right]\right\}\mathrm{d}x_1\int_{-b}^{b}\exp\left[ik\frac{(y-y_1)^2}{2z_1}\right]\mathrm{d}y_1$$

$$= \frac{\exp\left[ik(z_1+nd)\right]}{i\lambda z_1}U(x)\times V(y) \tag{9}$$

where

$$U(x) = \int_{-a}^{a}\exp\left\{ik\left[\frac{(x-x_1)^2}{2z_1}-(n-1)|x_1|\theta\right]\right\}\mathrm{d}x_1 \tag{10a}$$

$$V(y) = \int_{-b}^{b}\exp\left[ik\frac{(y-y_1)^2}{2z_1}\right]\mathrm{d}y_1 \tag{10b}$$

3.1. Exact evaluation of the diffraction integral

The exact evaluation of Eq. (9) can be given

$$E(x, y, z_1) = \frac{\exp\left[ik\left(z_1 - \frac{\alpha^2 z_1}{2}\right)\right]}{2i}\left\{\left[C(v_2) - C(v_1)\right] + i\left[S(v_2) - S(v_1)\right]\right\} \times$$

$$\times \left\{ \exp(-ik\alpha x)\left\{\left[C(u_{12}) - C(u_{11})\right] + i\left[S(u_{12}) - S(u_{11})\right]\right\} + \right.$$

$$\left. + \exp(ik\alpha x)\left\{\left[C(u_{22}) - C(u_{21})\right] + i\left[S(u_{22}) - S(u_{21})\right]\right\}\right\} \tag{11}$$

where C and S are the Fresnel integrals defined as

$$C(\tau) = \int_0^{\tau} \cos\left(\frac{\pi t^2}{2}\right) \mathrm{d}t \tag{12a}$$

$$S(\tau) = \int_0^{\tau} \sin\left(\frac{\pi t^2}{2}\right) \mathrm{d}t \tag{12b}$$

and

$$v_1 = \left(\frac{k}{\pi z_1}\right)^{1/2}(-b - y), \qquad v_2 = \left(\frac{k}{2\pi}\right)^{1/2}(b - y) \tag{13a}$$

$$u_{11} = \left(\frac{k}{\pi z_1}\right)^{1/2}(-x - \alpha z_1), \qquad u_{12} = \left(\frac{k}{\pi z_1}\right)^{1/2}(a - x - \alpha z_1) \tag{13b}$$

$$u_{21} = \left(\frac{k}{\pi z_1}\right)^{1/2}(x - \alpha z_1), \qquad u_{22} = \left(\frac{k}{\pi z_1}\right)^{1/2}(a + x - \alpha z_1) \tag{13c}$$

The integrals present in Eq. (9) and Eq. (11) do not have an analytical solution. To solve the diffraction integrals Eq. (9) and Eq. (11), we apply the stationary phase method to give an approximation representation and simulate the integrals with numerical calculation, respectively.

3.2. Evaluation diffraction integral by stationary phase method

To use the stationary phase approximation [4, 15], the corresponding integral $\boldsymbol{\Phi}$ that must be evaluated is of the following form:

$$\boldsymbol{\Phi} = \int_{w_1}^{w_2} g(r)\exp\left[ik\psi(r)\right]\mathrm{d}r \tag{14}$$

By the principle of a stationary phase, we know that if k is large enough, and $g(r)$ is slowly varying compared with the complex exponential, then the value of the integral $\boldsymbol{\Phi}$ which has an asymptotic representation in which the two lowest-order terms (*i.e.*, stationary U_S is proportional to $k^{-1/2}$ and edge U_E is proportional to k^{-1}), can be written as

$$\boldsymbol{\Phi} = U_S + U_E \tag{15}$$

where

$$U_S = \sqrt{\frac{2\pi}{k\left|\psi''(r_S)\right|}}\, g(r_S)\exp\left\{ik\psi(r_S) + \mathrm{sgn}\left[\psi''(r_S)\right]\frac{\pi}{4}\right\}, \qquad r_S \in (\omega_1, \omega_2) \tag{16a}$$

$$U_E = \frac{g(r)}{ik\psi'(r)}\exp\left[ik\psi(r)\right]\Big|_{\omega_1}^{\omega_2}, \qquad r_S \neq \omega_1 \vee \omega_2 \tag{16b}$$

while r_S denotes the stationary point of function $\Psi(r)$ which can be obtained from equation $\Psi'(r) = 0$.

According to the stationary phase method, the asymptotic representations of Eq. (10a) and Eq. (10b) can be given

$$V(y) = \sqrt{\lambda z_1}\exp\left(\frac{i\pi}{4}\right) + \frac{z_1}{k(b-y)}\exp\left[ik\frac{(b-y)^2}{2z_1} - \frac{i\pi}{2}\right] + \\ + \frac{z_1}{k(b+y)}\exp\left[ik\frac{(b+y)^2}{2z_1} - \frac{i\pi}{2}\right] \tag{17}$$

$$U(x) = \sqrt{\lambda z_1}\left\{\exp\left[-ik\left(\frac{\alpha^2 z_1}{2} - \alpha x\right) + \frac{i\pi}{4}\right] + \right. \\ \left. + \exp\left[-ik\left(\frac{\alpha^2 z_1}{2} + \alpha x\right) + \frac{i\pi}{4}\right]\right\} +$$

$$+\frac{z_1}{k(a-x-\alpha z_1)}\exp\left[ik\frac{(a-x)^2}{2z_1}-ik\alpha a-\frac{i\pi}{2}\right]+$$

$$+\frac{z_1}{k(a+x-\alpha z_1)}\exp\left[ik\frac{(a+x)^2}{2z_1}-ik\alpha a-\frac{i\pi}{2}\right] \tag{18}$$

Substituting Eq. (17) and Eq. (18) into Eq. (9), we can obtain the approximate complex-amplitude distribution of the diffractive field showed as

$$\begin{aligned}E(x,y,z_1) = \frac{\exp(ikz_1)}{i}\Bigg\{&\exp\left(\frac{i\pi}{4}\right)+\frac{\sqrt{\lambda z_1}}{2\pi(b-y)}\exp\left[ik\frac{(b-y)^2}{2z_1}-\frac{i\pi}{2}\right]+\\&+\frac{\sqrt{\lambda z_1}}{2\pi(b+y)}\exp\left[ik\frac{(b+y)^2}{2z_1}-\frac{i\pi}{2}\right]\Bigg\}\times\\\times\Bigg\{&\left\{\exp\left[-ik\left(\frac{\alpha^2 z_1}{2}-\alpha x\right)+\frac{i\pi}{4}\right]+\exp\left[-ik\left(\frac{\alpha^2 z_1}{2}+\alpha x\right)+\frac{i\pi}{4}\right]\right\}+\\&+\frac{\sqrt{\lambda z_1}}{2\pi(a-x-\alpha z_1)}\exp\left[ik\frac{(a-x)^2}{2z_1}-ik\alpha a-\frac{i\pi}{2}\right]+\\&+\frac{\sqrt{\lambda z_1}}{2\pi(a+x-\alpha z_1)}\exp\left[ik\frac{(a+x)^2}{2z_1}-ik\alpha a-\frac{i\pi}{2}\right]\Bigg\}\end{aligned} \tag{19}$$

where $0 < z_1 < D$. The terms of (19):

$$\frac{\sqrt{\lambda z_1}}{2\pi(b-y)}\exp\left[ik\frac{(b-y)^2}{2z_1}-\frac{i\pi}{2}\right] \tag{20a}$$

$$\frac{\sqrt{\lambda z_1}}{2\pi(b+y)}\exp\left[ik\frac{(b+y)^2}{2z_1}-\frac{i\pi}{2}\right] \tag{20b}$$

$$\frac{\sqrt{\lambda z_1}}{2\pi(a-x-\alpha z_1)}\exp\left[ik\frac{(a-x)^2}{2z_1}-ik\alpha a-\frac{i\pi}{2}\right] \tag{20c}$$

$$\frac{\sqrt{\lambda z_1}}{2\pi(a+x-\alpha z_1)}\exp\left[ik\frac{(a+x)^2}{2z_1}-ik\alpha a-\frac{i\pi}{2}\right] \tag{20d}$$

are the diffraction field caused by the edge of the rectangle aperture. Because $\sqrt{\lambda z_1}$ is small enough, we only consider the main terms. Equation (19) can be simplified as

$$E(x,y,z_1) = \exp\left(ikz_1-\frac{i\pi}{4}\right)\times \times\left\{\exp\left[-ik\left(\frac{\alpha^2 z_1}{2}-\alpha x\right)+\frac{i\pi}{4}\right]+\exp\left[-ik\left(\frac{\alpha^2 z_1}{2}+\alpha x\right)+\frac{i\pi}{4}\right]\right\} \tag{21}$$

The intensity distribution in the Fresnel zone $z_1 < D$ can be written as

$$I(x,y,z_1) = \left|E(x,y,z_1)\right|^2 = 2\left\{1+\cos\left[2k(n-1)\theta x\right]\right\} \tag{22}$$

which is the function of x, which has no relation with the observation distance z. The result is in accordance with the geometric optics analysis. With Equation (19) the field distribution features, such as, fringe space, focal length, intensity distribution, can be obtained directly. Equation (19) may help to analyze the diffraction impact on the field distribution. In order to evaluate the exact quality of the fringes, we use the numerical calculation to analyze the impact of diffractive field caused by the square edge on the fringes intensity distribution.

4. Numerical calculation and analysis

From Equation (6), we can see that the interference fringes intensity has sinusoidal distribution along the x direction and keeps invariable along the propagation direction. From Eq. (7), the fringes spacing which is proportional to the wavelength and reverse proportional to the refractive angle keeps equal at Fresnel area. The maximum focus segment can be obtained intuitively by the geometrical optics method. In Section 3, the scalar diffraction theory, with the paraxial approximation, is used to analyze the diffractive pattern generated by the square edges of the rectangle aperture. The approximation solution (Eq. (19)) of Fresnel integral given by the stationary phase method shows that the diffractive field consists of two parts, *i.e*., stationary term and square edges diffractive field. The analyzed results show that the fringes produced by thin biprism have non-diffraction property. Numerical calculation is applied to

investigate the non-diffraction property of the fringes and evaluate the influence of square edges diffractive field.

Based on Eq. (11) and the relation between the optical intensity and optical field, we can calculate the axial intensity of the focal segment as a function of z ($0 < z < D$). The calculations are made for $2a = 20$ mm, $2b = 20$ mm, $\lambda = 632.8$ nm, $\theta = 0.5°$, $n = 1.5$ and the focal segment D is equal to 2.2917 m. The theoretical fringes spacing is equal to 72.514 μm. Figure 3 shows the axial intensity in the diffractive field behind the biprism with the aperture size 20 mm×20 mm. Along the focal length, the intensity has a uniform distribution with a disturbance. The sharp oscillation around the average uniform intensity is caused by the diffraction of the sharp edges of the aperture, which could be depressed by apodization of the aperture [16].

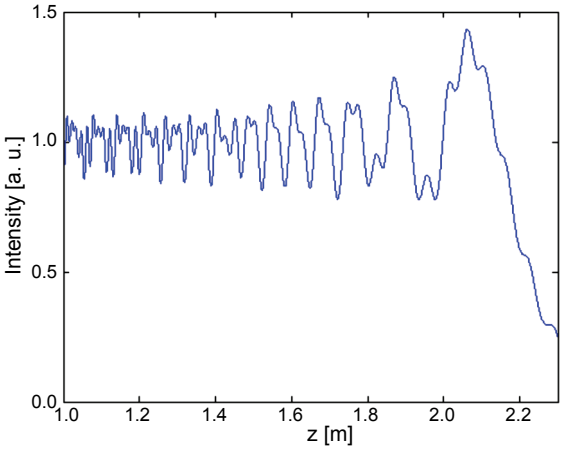

Fig. 3. Intensity distribution along z axial, $x = 0$, $y = 0$.

From Equation (6), we know that fringes intensity distribution keep invariable along the direction of propagation. Considering the diffractive effect, we calculate the intensity distribution along z axial from Eq. (11). The size of observation plane is $x \in [-0.5 \text{ mm}, 0.5 \text{ mm}]$, $y \in [-0.5 \text{ mm}, 0.5 \text{ mm}]$. Figure 4 shows the cross-section intensity distribution along X direction and the fringes spacing at different observation planes along Z axial. The little deviations of the fringes spacing calculated are caused by the numerical sampling error. The little disturbance of the intensity is induced by the diffractive field caused by the square edge. According to the numerical calculation result, the fringes generated by a plane wave illuminating the thin biprism have narrow spacing and long focal segment which have relation with the refractive angle, that is to say, the fringes have a non-diffraction property.

In order to evaluate the effect of the square edges diffractive field on the fringes intensity distribution, Eq. (19) is calculated with different aperture sizes. The disturbance is increased when the rectangle aperture size becomes small. The observation

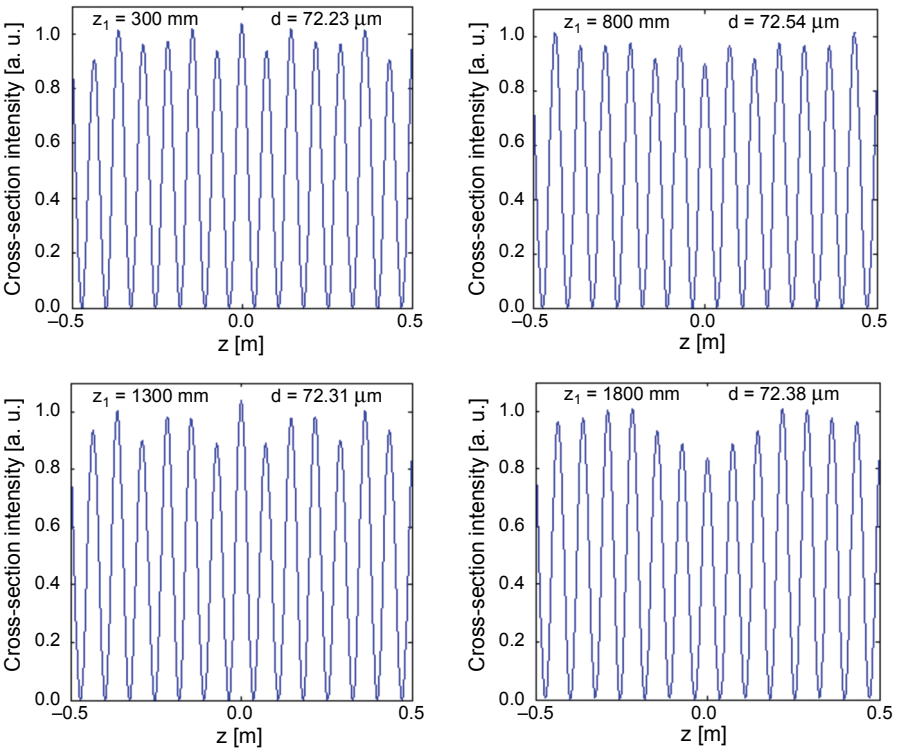

Fig. 4. Cross-section intensity distribution at different observation planes along *z* axial.

plane size is $x \in$ [–0.5 mm, 0.5 mm], $y \in$ [–0.5 mm, 0.5 mm]. Figure 5**a** shows the disturbance of the fringes intensity with the aperture size 20 mm×20 mm and Fig. 5**b** shows the disturbance of the fringes intensity with the aperture size 10 mm×10 mm. The other parameters of the thin biprism and incident light are the same. The standard deviations of the two conditions are 0.013 and 0.025, respectively.

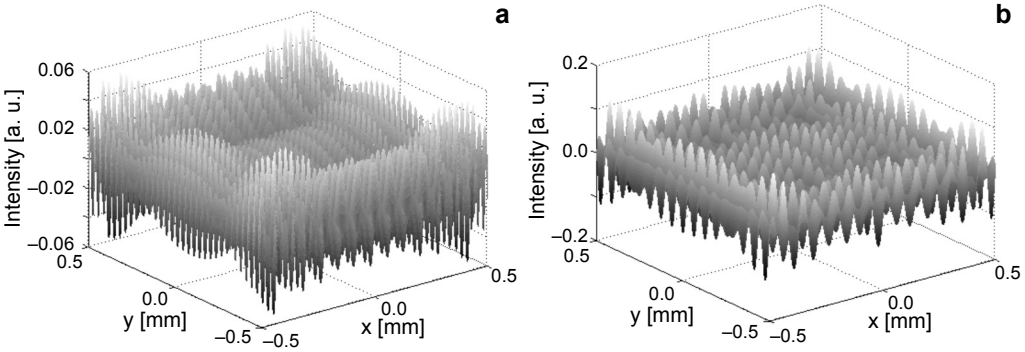

Fig. 5. Diffractive field caused by rectangle aperture edges. Rectangle aperture size is 20 mm×20 mm (**a**); and rectangle aperture size is 10 mm×10 mm (**b**).

5. Experimental results

Figure 6 gives the experimental setup to observe the fringes pattern. A beam from a He-Ne laser (wavelength 632.8 nm) is expanded and collimated to form a uniform monochromic plane wave, and then the plane wave illuminated the thin biprism (BK7, refractive angel 1.3° and rectangle aperture size 19.5 mm×20 mm). According to Eq. (7) and Eq. (5) the fringes spacing generated by this experimental setup is equal to 27.89 μm and the maximum focal segement is equal to 859.2 mm. The intensity distribution after the thin biprism is observed by COMS camera (pixel size 2.2 μm×2.2 μm) directly.

The intensity distribution is observed at a different distance and the fringes spacing is calculated which is showed in Tab. 1. The average spacing is 27.70 μm which is in accordance with the result calculated from Eq. (7). The result shows that the fringes spacing keep invariable along the light propagation direction. Figure 7 shows the central part intensity distribution on the observation plane at the distance z_1 = 100 mm

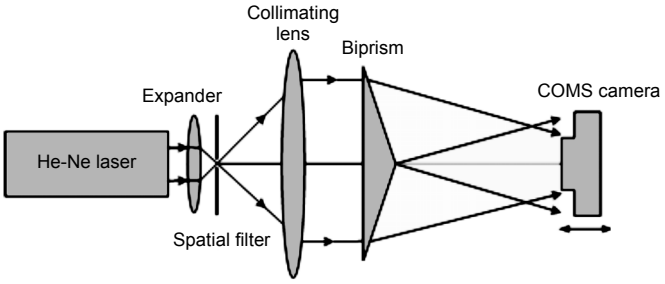

◀ Fig. 6. Experimental setup.

T a b l e 1. Fringes spacing at different observing distances from the biprism.

Distance [mm]	100	150	200	250	300	350	400	450	500	550	600
Spacing [μm]	27.72	27.70	27.67	27.67	27.53	27.79	27.73	27.70	27.56	27.82	27.82

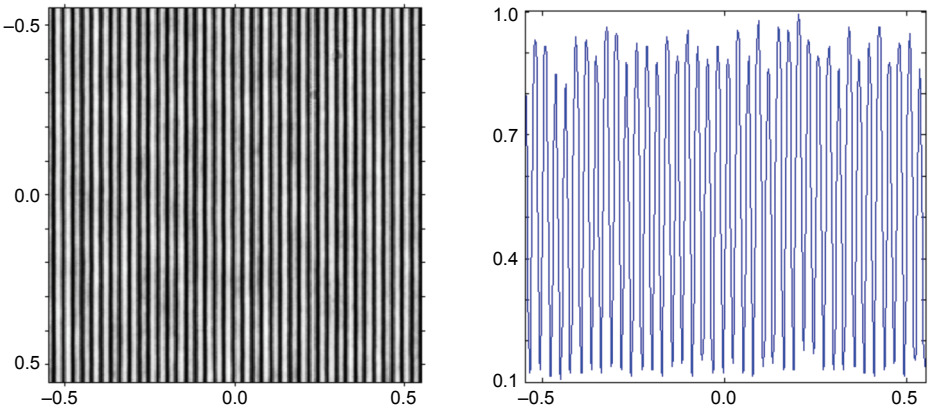

Fig. 7. Observed intensity at z_1 = 100 mm and cross-section intensity.

from the thin biprism, and the result is in accordance with the numerical calculation. The measured maximum focal length is equal to 850 mm. The fringes generated by this experimental setup have a non-diffraction characteristic.

6. Conclusions

We show the characteristics of non-diffraction fringes produced by a thin biprism when it is illuminated by a plane wave. The geometrical optical method and scalar diffraction theory, within the paraxial approximation, is used to analyze the property of the fringes produced by the thin biprism. The geometric optics analyzing approach can give direct field distribution features, such as, fringe space, focal length, intensity distribution. The diffraction optics analyzing approach can give a rigorous field distribution which may help to evaluate the impact of diffraction of the square edges of the rectangle aperture on the fringes intensity. These results are confirmed by the numerical evaluation of the Fresnel diffractive integral and experiments. The theoretical analysis, numerical simulation and experiments show that the fringes have a non-diffraction characteristic, *i.e*., the intensity distribution is invariable along the propagation direction z, the equal spacing is small and the focal length is large. The analysis method applied to evaluate the property of fringes intensity generated by the thin biprism can be utilized to design a proper biprism. The experimental setup to observe the non-diffraction fringes produced by the thin biprism is simple and compact, which may find potential applications in metrology.

Acknowledgements – The financial support provided by the National Natural Science Foundation of China (NSFC, No. 50975112).

References

[1] MCLEOD J.H., *The axicon: a new type of optical element*, Journal of the Optical Society of America **44**(8), 1954, p. 592.

[2] SOCHACKI J., BARA S., JAROSZEWICZ Z., KOLODZIEJCZYK A., *Phase retardation of the uniform-intensity axilens*, Optics Letters **17**(1), 1992, pp. 7–9.

[3] DAVIDSON N., FRIESEM A.A., HASMAN E., *Holographic axilens: high resolution and long focal depth*, Optics Letters **16**(7), 1991, pp. 523–525.

[4] JAROSZEWICZ Z., DOPAZO J.F.R., GOMEZ-REINO C., *Uniformization of the axial intensity of diffraction axicons by polychromatic illumination*, Applied Optics **35**(7), 1996, pp. 1025–1031.

[5] POPOV S.YU., FRIBERG A.T., *Apodization of generalized axicons to produce uniform axial line images*, Pure and Applied Optics: Journal of the European Optical Society Part A **7**(3), 1998, pp. 537–548.

[6] VASARA A., TURUNEN J., FRIBERG A.T., *Realization of general nondiffracting beams with computer-generated holograms*, Journal of the Optical Society of America A **6**(11), 1989, pp. 1748–1754.

[7] DAVIDSON N., FRIESEM A.A., HASMAN E., *Efficient formation of nondiffracting beams with uniform intensity along the propagation direction*, Optics Communications **88**(4–6), 1992, pp. 326–330.

[8] JIXIONG PU, HUIHUA ZHANG, SHOJIRO NEMOTO, WEIBIN ZHANG, WENZHEN ZHANG, *Annular-aperture diffractive axicons illuminated by Gaussian beams*, Journal of Optics A: Pure and Applied Optics **1**(6), 1999, pp. 730–734.

[9] PARKHOMENKO Y., SPEKTOR B., SHAMIR J., *Two regions of mode selection in resonators with biprism like elements*, Applied Optics **44**(13), 2005, pp. 2546–2552.

[10] JUNJI ENDO, JUN CHEN, DAI KOBAYASHI, YASUO WADA, HIROYUKI FUJITA, *Transmission laser microscope using the phase-shifting technique and its application to measurement of optical waveguides*, Applied Optics **41**(7), 2002, pp. 1308–1314.

[11] LOHMANN A.W., DAYONG WANG, PE'ER A., FRIESEM A.A., *Flatland optics. II. Basic experiments*, Journal of the Optical Society of America A **18**(5), 2001, pp. 1056–1061.

[12] YAOJU ZHANG, *Simple and rigorous analytical expression of the propagating field behind an axicon illuminated by an azimuthally polarized beam*, Applied Optics **46**(29), 2007, pp. 7252–7257.

[13] ZHANG Y., *Analytical expression for the diffraction field of an axicon using the ray-tracing and interference method*, Applied Physics B: Lasers and Optics **90**(1), 2008, pp. 93–96.

[14] PÉREZ M.V., GÓMEZ-REINO C., CUADRADO J.M., *Diffraction patterns and zone plates produced by thin linear axicons*, Optica Acta **33**(9), 1986, pp. 1161–1176.

[15] FRIBERG A.T., *Stationary-phase analysis of generalized axicons*, Journal of the Optical Society of America A **13**(4), 1996, pp. 743–750.

[16] JAROSZEWICZ Z., SOCHACKI J., KOLODZIEJCZYK A., STARONSKI L.R., *Apodized annular-aperture logatithmic axicon: smoothness and uniformity of intensity distributions*, Optics Letters **18**(22), 1993, pp. 1893–1895.

Receive October 27, 2011